

## Interfacial Free Energy Governs Single Polystyrene Chain Collapse in Water and Aqueous Solutions

Isaac T. S. Li and Gilbert C. Walker\*

Department of Chemistry, University of Toronto, Toronto, Ontario, Canada M5S 3H6

Received February 18, 2010; E-mail: gwalker@chem.utoronto.ca

**Abstract:** The hydrophobic interaction is significantly responsible for driving protein folding and self-assembly. To understand it, the thermodynamics, the role of water structure, the dewetting process surrounding hydrophobes, and related aspects have undergone extensive investigations. Here, we examine the hypothesis that polymer–solvent interfacial free energy is adequate to describe the energetics of the collapse of a hydrophobic homopolymer chain at fixed temperature, which serves as a much simplified model for studying the hydrophobic collapse of a protein. This implies that changes in polymer–solvent interfacial free energy should be directly proportional to the force to extend a collapsed polymer into a bad solvent. To test this hypothesis, we undertook single-molecule force spectroscopy on a collapsed, single, polystyrene chain in water–ethanol and water–salt mixtures where we measured the monomer solvation free energy from an ensemble average conformations. Different proportions within the binary mixture were used to create solvents with different interfacial free energies with polystyrene. In these mixed solvents, we observed a linear correlation between the interfacial free energy and the force required to extend the chain into solution, which is a direct measure of the solvation free energy per monomer on a single chain at room temperature. A simple analytical model compares favorably with the experimental results. This knowledge supports a common assumption that explicit water solvent may not be necessary for cases whose primary concerns are hydrophobic interactions and hydrophobic hydration.

### Introduction

The hydrophobic interaction is involved in many important chemical and biological processes including receptor–ligand interactions, protein folding and assembly, as well as interactions in lipid membranes. Understanding the mechanism of the hydrophobic effect has become increasingly important to explain fundamental biophysics and biochemistry<sup>1–7</sup> as well as to engineer new materials.<sup>8–12</sup> Despite the rich theoretical literature on hydrophobicity, the mechanism of the interaction is still not completely understood due to the relatively small amount of experimental verification. The effects of microscopic bubble

bridges,<sup>13,14</sup> water structure,<sup>15,16</sup> dewetting transition surrounding hydrophobes,<sup>17–19</sup> and solvent density fluctuation<sup>20–22</sup> have been investigated to explain the hydrophobic effect in various systems including particles,<sup>17,22</sup> plates,<sup>19,23</sup> proteins,<sup>2,24–29</sup> and polymers<sup>16,20,21,30,31</sup> (see reviews<sup>5,32–37</sup>). The role of hydrophobic interaction in the polymer and protein system is of special

- (1) Schlenoff, J. B.; Rmaile, A. H.; Bucur, C. B. *J. Am. Chem. Soc.* **2008**, *130*, 13589–13597.
- (2) Giovambattista, N.; Lopez, C. F.; Rosicky, P. J.; Debenedetti, P. G. *Proc. Natl. Acad. Sci. U.S.A.* **2008**, *105*, 2274–2279.
- (3) Honciuc, A.; Schwartz, D. K. *J. Am. Chem. Soc.* **2009**, *131*, 5973–5979.
- (4) Hummer, G.; Rasaiah, J. C.; Noworyta, J. P. *Nature* **2001**, *414*, 188–190.
- (5) Chandler, D. *Nature* **2005**, *437*, 640–647.
- (6) Liu, X. P.; Miller, M. J. S.; Joshi, M. S.; Thomas, D. D.; Lancaster, J. R. *Proc. Natl. Acad. Sci. U.S.A.* **1998**, *95*, 2175–2179.
- (7) Hummer, G.; Garde, S.; Garcia, A. E.; Paulaitis, M. E.; Pratt, L. R. *Proc. Natl. Acad. Sci. U.S.A.* **1998**, *95*, 1552–1555.
- (8) Giovambattista, N.; Debenedetti, P. G.; Rosicky, P. J. *Proc. Natl. Acad. Sci. U.S.A.* **2009**, *106*, 15181–15185.
- (9) Feng, X. J.; Feng, L.; Jin, M. H.; Zhai, J.; Jiang, L.; Zhu, D. B. *J. Am. Chem. Soc.* **2004**, *126*, 62–63.
- (10) Zhang, X.; Shi, F.; Yu, X.; Liu, H.; Fu, Y.; Wang, Z. Q.; Jiang, L.; Li, X. Y. *J. Am. Chem. Soc.* **2004**, *126*, 3064–3065.
- (11) Birois, S. M.; Ullrich, E. C.; Hof, F.; Trembleau, L.; Rebek, J. *J. Am. Chem. Soc.* **2004**, *126*, 2870–2876.
- (12) Guo, Z. G.; Zhou, F.; Hao, J. C.; Liu, W. M. *J. Am. Chem. Soc.* **2005**, *127*, 15670–15671.

- (13) Attard, P. *Langmuir* **2000**, *16*, 4455–4466.
- (14) Carambassis, A.; Jonker, L. C.; Attard, P.; Rutland, M. W. *Phys. Rev. Lett.* **1998**, *80*, 5357–5360.
- (15) Eriksson, J. C.; Henriksson, U. *Langmuir* **2007**, *23*, 10026–10033.
- (16) Goel, G.; Athawale, M. V.; Garde, S.; Truskett, T. M. *J. Phys. Chem. B* **2008**, *112*, 13193–13196.
- (17) Huang, X.; Margulis, C. J.; Berne, B. J. *Proc. Natl. Acad. Sci. U.S.A.* **2003**, *100*, 11953–11958.
- (18) Hummer, G.; Garde, S. *Phys. Rev. Lett.* **1998**, *80*, 4193–4196.
- (19) Huang, X. H.; Zhou, R. H.; Berne, B. J. *J. Phys. Chem. B* **2005**, *109*, 3546–3552.
- (20) ten Wolde, P. R.; Chandler, D. *Proc. Natl. Acad. Sci. U.S.A.* **2002**, *99*, 6539–6543.
- (21) Miller, T. F.; Vanden-Eijnden, E.; Chandler, D. *Proc. Natl. Acad. Sci. U.S.A.* **2007**, *104*, 14559–14564.
- (22) Willard, A. P.; Chandler, D. *J. Phys. Chem. B* **2008**, *112*, 6187–6192.
- (23) Choudhury, N.; Pettitt, B. M. *J. Am. Chem. Soc.* **2005**, *127*, 3556–3567.
- (24) Liu, P.; Huang, X. H.; Zhou, R. H.; Berne, B. J. *Nature* **2005**, *437*, 159–162.
- (25) Zhou, R. H.; Huang, X. H.; Margulis, C. J.; Berne, B. J. *Science* **2004**, *305*, 1605–1609.
- (26) Grater, F.; Heider, P.; Zangi, R.; Berne, B. J. *J. Am. Chem. Soc.* **2008**, *130*, 11578–11579.
- (27) Brylinski, M.; Konieczny, L.; Roterman, I. *Comput. Biol. Chem.* **2006**, *30*, 255–267.
- (28) Hummer, G.; Garde, S.; Garcia, A. E.; Paulaitis, M. E.; Pratt, L. R. *Biophys. J.* **1998**, *74*, A233–A233.
- (29) Cheung, M. S.; Garcia, A. E.; Onuchic, J. N. *Proc. Natl. Acad. Sci. U.S.A.* **2002**, *99*, 685–690.

interest due to the fact that the majority of functional biomolecules are polymeric. Because of the complex interactions involved in the hydrophobic collapse of polymers, it is difficult to directly apply the concept of hydrophobic interaction to study these systems of interest. In this study, we choose to explore how a simple parameter, namely the interfacial free energy between the hydrophobic polymer and solvents (interfacial free energy refers to polymer–solvent interfacial free energy for the rest of this article), can describe the force that holds a hydrophobic polymer chain (polystyrene) out of solutions: poor solvents for polystyrene. Indeed, theories and simulations studying the hydrophobic effect have used the solvent–vapor surface tension to predict the free energy of the interaction (surface tension refers to the liquid–vapor surface tension for the rest of this article). There is evidence that showed the solvation free energy of hydrophobic particles scale with the surface area.<sup>38</sup> However, some theories have predicted that this scaling law holds for large hydrophobic particles but fails for small hydrophobic particles where the solvation free energy scales with the volume.<sup>39–42</sup> In particular, it has been argued that the size of biological systems falls in the crossover region between small and large hydrophobic particles, making hydrophobic interaction's role there even more difficult to predict. In this article, we show from force–extension profile and solvent dependence data of a single polystyrene chain, that the system's solvation free energy scales with the length of the extended polymer, and the solvation free energy per monomer unit in aqueous solution is proportional to the interfacial free energy. At the same time, this does not contradict the size dependence effect predicted for small solutes.

Analytical theories and simulations have shown that a homopolymer in poor solvent under tension undergoes a phase transition where a single chain is forced to solvate by the external force as it is being pulled out of the collapsed state and into the solvent. When this happens, the collapsed state (beads) coexists with extended state (connecting thread) in a single chain in what is called the “necklace of beads” model where the force–extension profile in this transition region is constant.<sup>26,43–48</sup> In these models, the total free energy of the system is related to the solvent–solvent, polymer–solvent, and

polymer–polymer interactions; these effects are combined to give rise to the constant force profile. In the case of a hydrophobic polymer in aqueous solvents, the dominant driving force for the polymer collapse is the hydrophobic interaction. Therefore, the hydrophobic hydration of a polymer chain in solvent can be directly probed in the force plateau region. This is experimentally challenging as highly hydrophobic polymer does not dissolve in aqueous solvents, making it impossible to study with conventional ensemble measurements. However, it is possible to study such a system at a single molecule level where a single chain is pulled into solution by force spectroscopy using atomic force microscopy (AFM).

Force spectroscopy has become relatively commonplace during the past decade with the advancement of AFM, optical tweezers and other single molecule techniques. It has enabled numerous single molecule mechanical studies on biological molecules such as proteins and DNAs.<sup>49–52</sup> Much has been learned about the unfolding and refolding pathways of proteins under mechanical forces<sup>52–57</sup> as well as the binding activities between receptors and ligands<sup>58–60</sup> for example. Despite the numerous theoretical and simulation efforts, experimental studies focusing directly on hydrophobic collapse of polymers and proteins are still rare.<sup>61–65</sup> Due to the complex interactions of amino acids in proteins, it is difficult to isolate the role of hydrophobicity for study. Therefore in this work, we used a simple homopolymer whose primary apparent cause of collapse in water is the hydrophobic interaction. This facilitates theoretical modeling efforts and hence enables direct comparison of simulation and experiment. Although the polystyrene chain used in this experiment is a homopolymer and is roughly three times longer than that of a typical globular protein, it serves as a simple model for pulling hydrophobic chain from a single protein globule. The focus of the model here is to look at the effects of solvent conditions and how it affects the hydrophobic collapse from an energetic perspective. Single molecule force spectroscopy

- (30) Athawale, M. V.; Goel, G.; Ghosh, T.; Truskett, T. M.; Garde, S. *Proc. Natl. Acad. Sci. U.S.A.* **2007**, *104*, 733–738.
- (31) Hummer, G. *Proc. Natl. Acad. Sci. U.S.A.* **2007**, *104*, 14883–14884.
- (32) Berne, B. J.; Weeks, J. D.; Zhou, R. H. *Annu. Rev. Phys. Chem.* **2009**, *60*, 85–103.
- (33) ten Wolde, P. R. *J. Phys.: Condens. Matter* **2002**, *14*, 9445–9460.
- (34) Dill, K. A.; Truskett, T. M.; Vlachy, V.; Hribar-Lee, B. *Annu. Rev. Biophys. Biomol.* **2005**, *34*, 173–199.
- (35) Pratt, L. R. *Annu. Rev. Phys. Chem.* **2002**, *53*, 409–436.
- (36) Rasaiah, J. C.; Garde, S.; Hummer, G. *Annu. Rev. Phys. Chem.* **2008**, *59*, 713–740.
- (37) Ball, P. *Chem. Rev.* **2008**, *108*, 74–108.
- (38) Ashbaugh, H. S.; Kaler, E. W.; Paulaitis, M. E. *J. Am. Chem. Soc.* **1999**, *121*, 9243–9244.
- (39) Huang, D. M.; Chandler, D. *Proc. Natl. Acad. Sci. U.S.A.* **2000**, *97*, 8324–8327.
- (40) Lum, K.; Chandler, D.; Weeks, J. D. *J. Phys. Chem. B* **1999**, *103*, 4570–4577.
- (41) Huang, D. M.; Chandler, D. *J. Phys. Chem. B* **2002**, *106*, 2047–2053.
- (42) Rajamani, S.; Truskett, T. M.; Garde, S. *Proc. Natl. Acad. Sci. U.S.A.* **2005**, *102*, 9475–9480.
- (43) Dobrynin, A. V.; Rubinstein, M.; Obukhov, S. P. *Macromolecules* **1996**, *29*, 2974–2979.
- (44) Pickett, G. T.; Balazs, A. C. *Langmuir* **2001**, *17*, 5111–5117.
- (45) Halperin, A.; Zhulina, E. B. *Macromolecules* **1991**, *24*, 5393–5397.
- (46) Cooke, I. R.; Williams, D. R. M. *Europhys. Lett.* **2003**, *64*, 267–273.
- (47) Zhulina, E.; Walker, G. C.; Balazs, A. C. *Langmuir* **1998**, *14*, 4615–4622.
- (48) Halperin, A.; Zhulina, E. B. *Europhys. Lett.* **1991**, *15*, 417–421.

- (49) Smith, S. B.; Finzi, L.; Bustamante, C. *Science* **1992**, *258*, 1122–1126.
- (50) Kellermayr, M. S. Z.; Smith, S. B.; Granzier, H. L.; Bustamante, C. *Science* **1997**, *276*, 1112–1116.
- (51) Rief, M.; Gautel, M.; Oesterhelt, F.; Fernandez, J. M.; Gaub, H. E. *Science* **1997**, *276*, 1109–1112.
- (52) Marszalek, P. E.; Lu, H.; Li, H. B.; Carrion-Vazquez, M.; Oberhauser, A. F.; Schulten, K.; Fernandez, J. M. *Nature* **1999**, *402*, 100–103.
- (53) Meadows, P. Y.; Bemis, J. E.; Walker, G. C. *Langmuir* **2003**, *19*, 9566–9572.
- (54) Best, R. B.; Fowler, S. B.; Toca-Herrera, J. L.; Clarke, J. *Proc. Natl. Acad. Sci. U.S.A.* **2002**, *99*, 12143–12148.
- (55) Ng, S. P.; Rounsevell, R. W. S.; Steward, A.; Geierhaas, C. D.; Williams, P. M.; Paci, E.; Clarke, J. *J. Mol. Biol.* **2005**, *350*, 776–789.
- (56) Mitternacht, S.; Luccioli, S.; Torcini, A.; Imparato, A.; Irback, A. *Biophys. J.* **2009**, *96*, 429–441.
- (57) Li, H.; Oberhauser, A.; Fowler, S.; Clarke, J.; Marszalek, P. E.; Fernandez, J. M. *Biophys. J.* **2000**, *78*, 402a–402a.
- (58) Merkel, R.; Nassoy, P.; Leung, A.; Ritchie, K.; Evans, E. *Nature* **1999**, *397*, 50–53.
- (59) Moy, V. T.; Yuan, C.; Chen, A.; Kolb, P. *Mol. Biol. Cell* **1999**, *10*, 75a–75a.
- (60) Marshall, B. T.; Sarangapani, K. K.; Lou, J. H.; McEver, R. P.; Zhu, C. *Biophys. J.* **2005**, *88*, 1458–1466.
- (61) Gunari, N.; Walker, G. C. *Langmuir* **2008**, *24*, 5197–5201.
- (62) Gunari, N.; Balazs, A. C.; Walker, G. C. *J. Am. Chem. Soc.* **2007**, *129*, 10046–10047.
- (63) Kiriy, A.; Gorodyska, G.; Minko, S.; Jaeger, W.; Stepanek, P.; Stamm, M. *J. Am. Chem. Soc.* **2002**, *124*, 13454–13462.
- (64) Walther, K. A.; Grater, F.; Dougan, L.; Badiella, C. L.; Berne, B. J.; Fernandez, J. M. *Proc. Natl. Acad. Sci. U.S.A.* **2007**, *104*, 7916–7921.
- (65) Yasuda, S.; Suzuki, I.; Shinohara, K.; Shigekawa, H. *Phys. Rev. Lett.* **2006**, *96*, 228303.

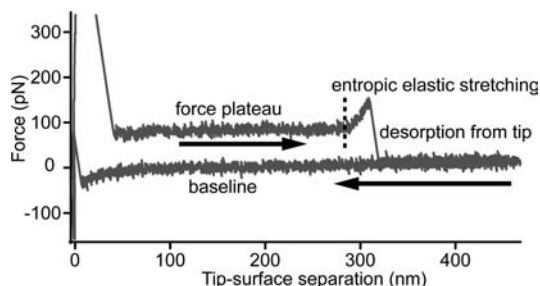


**Figure 1.** A typical force–extension curve in an AFM pulling experiment. The arrow pointing left indicates the motion of the cantilever as it approaches the surface where a single polymer physisorbs onto the tip and the arrow pointing right illustrates the motion of the cantilever as it moves away from the surfaces, pulling this polymer chain with it. The tip–surface separation is the experimental coordinate for polymer extension. The part of the force–extension curve that is parallel to the baseline is the force plateau region, followed by an entropically elastic region where the force rises before the polymer detaches from the cantilever tip.

copy allows us to observe the force response of a single molecule under mechanical perturbation.

In this paper we report single-molecule pulling experiments on polystyrene in various aqueous solvents. The results show a linear correlation between the force to extend the hydrophobic polymer and the polymer–solvent interfacial free energy obtained from macroscopic measurement. Our analytical model confirms the experimental results by showing similar force–extension profiles and linear dependency of the extension force to the interfacial free energy. These results suggest that, fixed at room temperature, the macroscopically measured interfacial free energy between polystyrene polymer and aqueous solvent captures most of the essential interactions that are still applicable to microscopic systems down to a single macromolecule.

## Methods and Materials

**Sample Preparation.** Polystyrene with a molecular weight of 130k and a polydispersity of 1.05 was purchased from Polymer Source (P5157-S). The polymer was dissolved in distilled tetrahydrofuran (Sigma Aldrich) or toluene (Sigma Aldrich) at 1 mg/mL concentration for 6 h and subsequently diluted to 1  $\mu$ g/mL and left to further dissolve for 24 h. The diluted solution was then spin-coated on a piranha-cleaned silicon wafer or flame-annealed gold at 2000 rpm for 1 min. The sample was then thoroughly dried in a vacuum chamber before use. Ethanol and deionized water were passed through 0.2  $\mu$ m PTFE and cellulose filters, respectively. The mixing volume was determined on the basis of the densities of both solvents at room temperature.

**Single-Molecule Force Spectroscopy.** Gold-coated biolevers from Olympus (BL-RC150VB-C1) and silicon nitride cantilevers from Veeco (MLCT-AUNM) were used in the single-molecule pulling experiments. The cantilever spring constants were calibrated by thermal method, and are  $\sim$ 5 pN/nm and  $\sim$ 15 pN/nm, respectively. All experiments were performed using the MFP-3D AFM from Asylum Research. For all experiments, the system temperature was kept constant at 300 K using the thermal controller from Asylum Research. The data acquisition rate was 5 kHz, and various pulling velocities between 500 and 3000 nm/s were used. Data were analyzed by custom scripts written in Igor Pro 6.12 (Wavemetrics).

## Results and Discussion

**Typical Force–Extension Profile of Polystyrene in Water.** A typical force–extension curve of polystyrene in water is shown in Figure 1. In each pulling cycle, the AFM cantilever is first lowered toward and makes contact with the surface, then is moved away from the surface. While the tip of the cantilever

is in close proximity to the surface, part of a polystyrene molecule may physisorb onto the tip apex and subsequently be stretched between the surface and the tip apex. The force–extension profile shows a force plateau region followed by a short entropically elastic region before the chain desorbs from the tip. The force plateau region corresponds to the chain undergoing the transition from collapsed to extended state where collapsed and extended structures coexist in the same molecule. The force to extend the polymer is constant because the change in free energy is proportional to the polymer–solvent contact area, which is proportional to the length of the extended (solvent-exposed) state of the polymer. As the chain is extended further, the percentage of collapsed structure in the chain drops until the whole chain is solvent-exposed; beyond this point, the force–extension profile of the chain can be characterized by entropic elasticity. A short-range repulsive force was observed as the tip approaches to within roughly 50 nm from the surface. This short-range repulsive force was observed only when using deionized water and disappears if trace amount of salt is added, indicating that this was likely due to charge accumulation at the surface of silicon, and that the repulsion is electrostatic. The cantilever also experiences a surface adhesion force before it snaps off from surface while the cantilever is moving away from the surface. The adhesion and snap-off prevents observation of the force–extension response of the chain at short extension lengths.

**Analytical Model of Pulling a Single Chain from Collapsed State.** We provide a simple analytical model that captures most of the physics in pulling a polymer in bad solvent from a collapsed to an extended state. This model is built upon the model of Halperin and Zhulina<sup>45,48</sup> that yields a collapsed–extended coexistence state before reaching the fully solvent-exposed state. Several modifications were made to suit this model to our systems (see Figure 2a). Instead of assuming the extended state is composed of smaller-sized collapsed blobs on a Gaussian chain, here we model the extended state as a single worm-like-chain (WLC) with a constant diameter. The collapsed state is modeled as a sphere with a size at least 10 times greater than the diameter of the chain. The total volume of the sphere and the flexible rod is conserved:

$$V = \frac{4}{3}\pi R^3 + \pi r^2 L \quad (1)$$

where  $R$  is the radius of the collapsed sphere,  $r$  is the radius of the rod modeling the single chain, and  $L$  is the contour length of the extended component of the chain. While holding the end of the extended component at a fixed distance, an intricate balance of forces at the interface occurs between the collapsed and extended component of the chain. At the interface, the entropic elastic force from the extended single-chain component balances the force that pushes the extended component back into the collapsed component due to the solvophobic effect. We use the worm-like-chain model<sup>66,67</sup> to obtain the force from the entropic elasticity of the extended component of the chain:

$$F_{\text{WLC}} = \frac{k_B T}{L_p} \left[ \frac{1}{4} \left( 1 - \frac{x}{L} \right)^{-2} - \frac{1}{4} + \frac{x}{L} \right] \quad (2)$$

where  $L_p$  is the persistence length of the chain. Similar to the Halperin–Zhulina model,<sup>45,48</sup> we assume the change in solvation free energy is proportional to the change in interfacial area and free energy between the polymer and solvent. Assuming the first derivative of force–extension curve is continuous, the



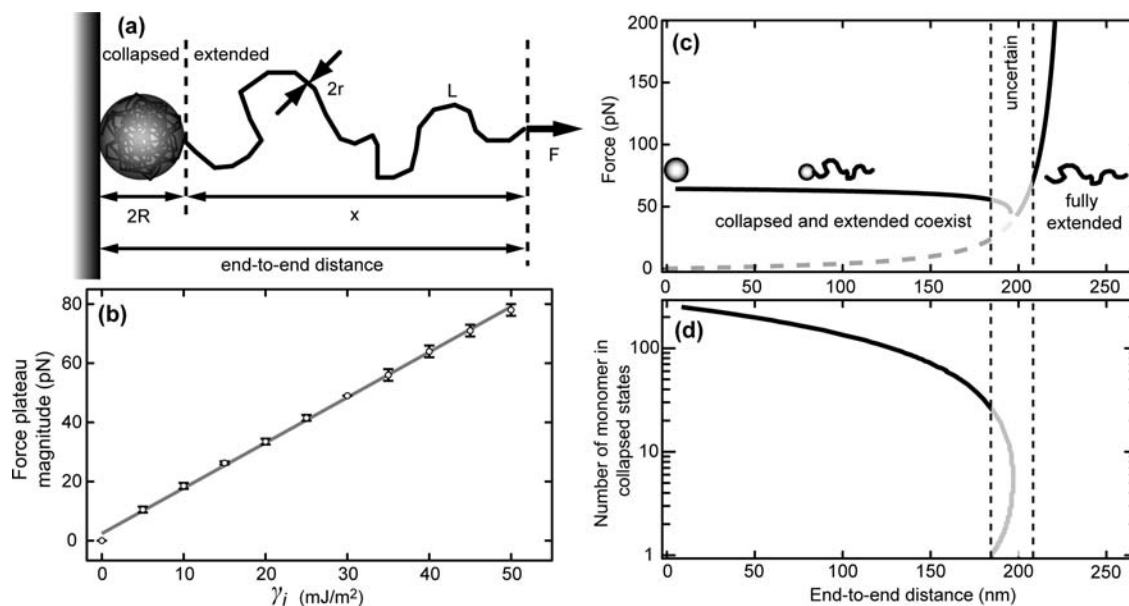


**Figure 2.** Simple analytical model and results. (a) Illustration of the pulling experiment, the coexistence of collapsed and extended state in the same polymer as well as the entropic elastic response of the extended state.  $R$  is the radius of the collapsed sphere,  $r$  is the radius of the single chain modeled as a flexible rod,  $L$  is the contour length of the extended single chain,  $x$  is the end-to-end distance of the extended single chain, and  $F$  is the force applied to the single chain. (b) Illustrates the plateau force calculated from the analytical model against the interfacial free energy used in the calculation. (c, d) Predictions of the analytical model: (c) force–extension profile using the model, (d) number of monomers in the collapsed sphere in log scale. The grayed-out uncertain area indicates regions where there will be a failure of the assumption that the collapsed state will remain spherical when there are only a small number of monomers in the collapsed state.

change in solvation energy of the system should equal to the work done by the entropic elasticity if  $x$  changes by an infinitesimal amount  $dx$ :

$$F_{\text{WLC}} dx = \gamma_i dA \quad (3)$$

$$A = 4\pi R^2 + 2\pi rL \quad (4)$$

where  $\gamma_i$  is the interfacial free energy between the polymer chain and the solvent,  $A$  is the total surface area of the polymer including the collapsed and extended components. This is then simplified to:

$$F_{\text{WLC}} \frac{x}{L} = 2\pi r \gamma_i \left(1 - \frac{r}{R}\right) \quad (5)$$

By parametrizing  $x$  and  $F_{\text{WLC}}$  with  $\varphi = x/L$  (see Supporting Information), we were able to obtain numerical solutions to this complex equation with the parameters listed in Table 1.

$$x(\varphi) = \frac{V}{\pi r^2 \varphi} - \frac{4r}{3 \left(1 - \frac{F_{\text{WLC}}(\varphi) \varphi}{2\pi r \gamma_i}\right)^3 \varphi} \quad (6)$$

$$F_{\text{WLC}}(\varphi) = \frac{k_B T}{L_p} \left[ \frac{1}{4} (1 - \varphi)^{-2} - \frac{1}{4} + \varphi \right]$$

$$\varphi = \frac{x}{L}$$

Using parameters from Table 1, the force–extension profile from this model shows a well-defined plateau with a slight negative slope toward higher extension at roughly 1.8 pN per 100 nm of extension (Figure 2c). The assumption that the

**Table 1.** List of Parameters Used in the Analytical Model

parameter	value
$\gamma_i$	40.0 mJ/m <sup>2</sup>
$V$	$4.7 \times 10^{-26}$ m <sup>3</sup>
$r^a$	0.25 nm
number of monomers	1000
length per monomer	0.24 nm
$L_p$	0.92 nm
$T$	300 K

<sup>a</sup> The radius of the cylinder is a crude estimate based on the size of a styrene molecule using bond lengths and simple geometry. This is only meant to give the approximate order of magnitude and not the exact value for the force opposing polystyrene extension.

collapsed sphere is much greater in size than the diameter of the extended worm-like-chain begins to fail toward higher extension length when the number of monomers in the collapsed state is on the order of 10's; this model cannot accurately predict the force–extension response in the transition from the collapsed–extended coexistence state to the fully extended state (indicated as the “uncertain” region in Figure 2c, d). Beyond the transition region, the chain has no collapsed component and shows only the entropic elastic response. The plateau force region is where the collapsed and extended components coexist within the polymer chain. The magnitude of the constant force in the plateau region is nearly entirely contributed by the solvation of chain from collapsed to extended state and is therefore proportional to solvent-exposed area and the interfacial free energy between the polymer and the solvent. As shown in Figure 2b, the force plateau magnitude can be linearly related to the interfacial free energy by:

$$F_{\text{plateau}} = (1.53 \pm 0.04) \gamma_{\text{PS-sol}} + (2 \pm 1) \text{ [pN]} \quad (7)$$

where  $\gamma_{\text{PS-sol}}$  has the unit of mJ/m<sup>2</sup>.

As will be discussed below, the AFM experiment provides similar linear correlation between the plateau force magnitude

(66) Bustamante, C.; Marko, J. F.; Siggia, E. D.; Smith, S. *Science* **1994**, *265*, 1599–1600.

(67) Marko, J. F.; Siggia, E. D. *Macromolecules* **1995**, *28*, 8759–8770.

and the polystyrene-solvent interfacial free energy. The model would produce similar results if there were more than one collapsed components along a single chain, for example one adsorbed onto the AFM tip and another one adsorbed onto the surface or more than one suspended between the tips. However, more realistically, many smaller collapsed components are not as favored energetically as few, larger ones on a single chain. Therefore, it is expected that the smaller collapsed components will dissolve and contribute to create a single, larger, collapsed state.

This model does not take into account the elastic response from the collapsed component of the chain because it is assumed the collapsed state is much larger in size comparing to the worm-like-chain. If a very large collapsed component size is assumed, the change in surface area caused by the external force is relatively small compared to the total area of the collapsed state, and hence can still be approximated by a sphere. The deformation of the collapsed component modeled by Halperin and Zhulina is limited only to the region before the extended-collapsed coexistence state. Since the initial deformation is not the focus of the current discussion, this was neglected from our model. However, we are interested in the effect of the collapsed component deformation in our finite sized system at the coexistence stage of the extension. One can imagine that, under tension, the collapsed component would be elongated to an ellipsoidal shape rather than a perfectly spherical shape. This ellipsoidal geometry increases the surface area of the collapsed component which would have an impact on the force-extension profile. At the same distortion force, the degree of distortion would be greater on a smaller collapsed component than on a larger one due to less interchain interactions. Therefore, this model's assumption of a spherical collapsed component at all stages of the extension has underestimated the surface area of collapsed component, and therefore the total solvent-exposed area of the whole polymer. Toward higher extension the increase of solvent-exposed area is further underestimated as the solvent-exposed area of the collapsed component is increased due to a higher degree of deformation. Hence, the force is also underestimated at higher extension in the collapse-extended coexistence state. Therefore, the elastic distortion of the collapsed component could ease the negative slope of the force-extension plateau if it were incorporated in the model. Here we do not include this effect for two reasons: (1) we cannot estimate the elastic response of the collapsed component in a simple way, and (2) the current model captures the main behavior.

Another aspect to consider, given recent developments of hydrophobic theory, is the size effect of the hydrophobic solute.<sup>39,40</sup> It has been shown that the solvation free energy of small hydrophobic particles on the order of several angstroms do not scale with a particle's surface area, but rather with its volume. This lowers the solvation free energy of small solutes when comparing to what one would expect if it were to scale with the former. If this indeed applies to the solvation of each monomer along the polymer chain, a scaling factor could be added to eq 6, which would influence the magnitude of the plateau force, but not the overall shape of the force-extension profile. This is because the solvation free energy per monomer is identical; therefore, the total solvation free energy of  $N$  monomer units would be proportional to  $N$ , which in the case of the linear polymer is also directly proportional to the length of the extended chain. Thus, the size effect is applicable to the individual monomers along the chain and hence does not alter

the key features of the model. To illustrate this more clearly, we consider this simple equation:

$$E_{\text{total}} = \alpha(R)N\gamma_{\text{PS-solvent}} \quad (8)$$

where  $E_{\text{total}}$  is the total solvation free energy of the extended chain,  $N$  is the length of the extended chain in number of monomers,  $\alpha(R)$  is a size-dependent, effective surface area per monomer, and  $\gamma_{\text{PS-solvent}}$  is the polymer-solvent interfacial free energy. The force plateau in experiment force curves (Figure 1) confirms that the total solvation free energy of the extended chain is proportional to length:

$$E_{\text{total}} \propto N \quad (9)$$

By varying solvent conditions, i.e. the main thrust of the article in the following text, we find that the solvation free energy per monomer is linearly dependent on the polymer-solvent interfacial free energy:

$$\frac{E_{\text{total}}}{N} \propto \gamma_{\text{PS-solvent}} \quad (10)$$

The value of  $\alpha(R)$  can be obtained from the slope from plotting  $E_{\text{total}}/N$  against  $\gamma_{\text{PS-solvent}}$  as will be shown later in the text.

Whether the solvation of individual monomers on a polymer chain is strongly size dependent is still debated: when extended, a polymer is a macroscopic object in the dimension along the chain, and obeys a surface area dependent scaling law, but it is microscopic in the radial direction, where a hydrophobic size effect might play a role. Therefore, the solvation free energy of each monomer on the polymer may not be simply equated to the solvation free energy of the monomer alone in the solvent.

**Interfacial Free Energy between Polystyrene and Various Solvents.** We hypothesized that the force plateau is due to hydrophobic hydration, and the magnitude of the plateau force is therefore proportional to the interfacial free energy between the aqueous solvent and the polymer. To test this hypothesis, we performed pulling experiments on single polystyrene molecules adsorbed on silicon surface in different aqueous solvents. Different PS-solvent interfacial free energy  $\gamma_{\text{PS-sol}}$  can be achieved by changing solvent surface tension and can be calculated according to the extended Fowkes equation:<sup>68-72</sup>

$$\gamma_{\text{PS-sol}} = \gamma_{\text{PS}} + \gamma_{\text{sol}} - 2\sqrt{\gamma_{\text{PS}}^{\text{d}}\gamma_{\text{sol}}^{\text{d}}} - 2\sqrt{\gamma_{\text{PS}}^{\text{p}}\gamma_{\text{sol}}^{\text{p}}} \quad (11)$$

or Wu's equation:<sup>73,74</sup>

$$\gamma_{\text{PS-sol}} = \gamma_{\text{PS}} + \gamma_{\text{sol}} - \left( \frac{4\gamma_{\text{PS}}^{\text{d}}\gamma_{\text{sol}}^{\text{d}}}{\gamma_{\text{PS}}^{\text{d}} + \gamma_{\text{sol}}^{\text{d}}} \right) - \left( \frac{4\gamma_{\text{PS}}^{\text{p}}\gamma_{\text{sol}}^{\text{p}}}{\gamma_{\text{PS}}^{\text{p}} + \gamma_{\text{sol}}^{\text{p}}} \right) \quad (12)$$

with

$$\gamma_{\text{PS}} = \gamma_{\text{PS}}^{\text{d}} + \gamma_{\text{PS}}^{\text{p}} \quad (13)$$

$$\gamma_{\text{sol}} = \gamma_{\text{sol}}^{\text{d}} + \gamma_{\text{sol}}^{\text{p}} \quad (14)$$

where  $\gamma_{\text{PS}}$  and  $\gamma_{\text{sol}}$  are the surface tensions of polystyrene and the solvent,  $\gamma_{\text{PS}}^{\text{d}}$  and  $\gamma_{\text{sol}}^{\text{d}}$  are the dispersive contributions to the

(68) Fowkes, F. M. *J. Phys. Chem.* **1962**, *66*, 382-382.

(69) Good, R. J.; Girifalco, L. A. *J. Phys. Chem.* **1960**, *64*, 561-565.

**Table 2.** Dispersive and Polar Contributions to Surface Tensions of the Solvent Used in This Study As Well As the Interfacial Free Energy between the Solvent and Polystyrene

solvent	$\gamma_{\text{sol}}^{\text{d}}$ (mJ/m <sup>2</sup> )	$\gamma_{\text{sol}}^{\text{p}}$ (mJ/m <sup>2</sup> )	$\gamma_{\text{sol}}^{\text{p}}$ (mJ/m <sup>2</sup> )	$\gamma_{\text{PS-sol}}^{\text{p}}$ (mJ/m <sup>2</sup> )
Poor Solvents				
2 M NaCl in water <sup>79,80</sup>	76.8	22.1	54.7	43.6
water <sup>77</sup>	72.6	22.1	50.6	40.0
2.5 mol % EtOH <sup>77</sup>	57.6	20.6	37.0	29.0
5.0 mol % EtOH <sup>77</sup>	47.7	19.6	28.1	22.1
10 mol % EtOH <sup>77</sup>	36.8	18.5	18.3	14.7
20 mol % EtOH <sup>77</sup>	29.5	17.8	11.8	10.2
30 mol % EtOH <sup>77</sup>	27.6	17.6	10.0	9.1
40 mol % EtOH <sup>77</sup>	26.6	17.5	9.1	8.5
EtOH <sup>77</sup>	21.9	17.0	4.9	6.2
Good Solvents				
iodomethane <sup>81</sup>	45.0	42.1	2.9	0.5
hexadecane <sup>82</sup>	27.6	27.6	0.0	2.0
benzene	28.9	28.9	0.0	1.8

polymer	$\gamma_{\text{PS}}^{\text{d}}$ (mJ/m <sup>2</sup> )	$\gamma_{\text{PS}}^{\text{p}}$ (mJ/m <sup>2</sup> )	$\gamma_{\text{PS}}^{\text{p}}$ (mJ/m <sup>2</sup> )	
polystyrene <sup>75</sup>	40.7	35.9	4.8	derived from Wu's eq
polystyrene <sup>75</sup>	40.6	39.7	0.9	derived from ext. Fowkes eq

surface tensions,  $\gamma_{\text{PS}}^{\text{p}}$  and  $\gamma_{\text{sol}}^{\text{p}}$  are the polar contributions to the surface tensions of PS and the solvent.

The dispersion and polar components of polystyrene have been reported with great variations, which is also the case for many other polymers.<sup>75,76</sup> The discrepancy in the reported dispersion and polar component values can be a result of the model or equation used to produce them. For instance, in the study by Saito,<sup>75</sup> the polar component of polystyrene of 0.9 mJ/m<sup>2</sup> was generated using the extended Fowkes equation whereas the polar component is 4.8 mJ/m<sup>2</sup>, over 5 times greater when generated using Wu's equation (see Table 2).<sup>75</sup> Since both values are calculated from the same experimental contact angle measurements, they should reproduce the same work of adhesion with the corresponding equations. The discrepancies in polar and dispersive contributions from the two equations are entirely due to their different definitions in the work of adhesion calculation. Hence, as long as the equation used to calculate the interfacial free energy matches the one used to obtain the polar and dispersive contributions, these discrepancies will not affect the interfacial free energy. In this study, the solvent polar and dispersive components from literature<sup>75,77</sup> are calculated using the extended Fowkes equation; to match it, we use the polar and dispersive components of polystyrene calculated also by the extended Fowkes equation (see Table 2).

Decreasing the surface tension of the aqueous solution most effectively reduces the interfacial free energy with the polymer. To reduce the surface tension of the aqueous solution in the experiment, we added ethanol to deionized water at different molar ratios (see Table 2). The addition of ethanol to water strongly influences the surface tension of water, giving surface tensions that range from 72.6 to 21.9 mJ/m<sup>2</sup>. It has been reported that ethanol reduces the surface tension of water by changes in hydrophobic hydration.<sup>78</sup> The dispersive and polar contributions to the surface tension of ethanol–water mixture were taken from earlier contact angle experiments.<sup>77</sup> It has been shown that addition of salt increases the surface tension of the water by a combination of factors including the electrostatic image force, ion hydration, and others as described by Weissenborn.<sup>79,80</sup> For NaCl in water, the surface tension increases by 2.08 mJ/m<sup>2</sup> for every additional molar increase in the concentration of NaCl.<sup>79,80</sup> Higher surface tension does not necessarily result in higher interfacial free energy; Table 2 shows that iodomethane has a large surface tension but a low interfacial free energy. Apparently the boundary between good and bad solvent for polystyrene occurs at an interfacial free energy of  $\sim 5$  mJ/m<sup>2</sup>.

The addition of ethanol or salt affects mainly the polar component of solution surface tension, while the dispersion component does not vary much. At the same time, the polar component of the surface energy of polystyrene according to the extended Fowkes equation contributes only 2.2% of the total adhesive interaction energy between polystyrene and the various solvents, while the rest comes from dispersive interactions (Table 2). This indicates that the change in interfacial free energy contributed by dispersive interaction is relatively constant for our aqueous solutions, while the greatest contribution comes from the changes in the polar component of the solvent. Since the polar interaction and hydrogen bonding in aqueous solution is the putative cause of hydrophobic effect, this result suggests that, by adding ethanol and salt, one is directly modifying the strength of hydrophobic hydration and hydrophobic interaction.

**Single-Molecule Pulling of Polystyrene in Aqueous Solutions of Ethanol and NaCl.** Varying the concentration of ethanol in water changes the surface tension of the solution and consequently changes the interfacial free energy between the polymer and the solvent. All experiments were done in a closed fluid cell, to minimize solvent evaporation that would lead to changes in concentration of ethanol and NaCl. Force plateaus were seen in pulling experiments in all water–ethanol mixtures and pure ethanol (Figure 3). We find that with increasing ethanol content, the plateau force decreases (Figure 3), while NaCl salt solution elevates the plateau force (Table 3). To find the magnitude of the plateau forces more accurately, we overlapped the force curves from each solvent experiment by their retraction baseline (Figure 4a) and created a histogram of forces from regions of the force–extension curve that contains only the force plateaus (i.e., no indentation) and the retraction baseline (Figure 4b). The retraction baseline is used because the cantilever is moving at the same velocity in the force plateau region as in the retraction baseline. As will be described later in the article, the force plateau is also velocity independent over the range studied. Hence, there is no need to correct for any effects due to pulling velocity. The histogram containing only the plateau and baseline is then fitted to Gaussian curves to assess the mean and standard deviations of the plateau force (Figure 4b).

(70) Owens, D. K. *J. Appl. Polym. Sci.* **1970**, *14*, 1725–1730.

(71) Fowkes, F. M. *J. Phys. Chem.* **1963**, *67*, 2538–2541.

(72) Fowkes, F. M. *Ind. Eng. Chem.* **1964**, *56*, 40–52.

(73) Wu, S. J. *Colloid Interface Sci.* **1969**, *31*, 153–161.

(74) Wu, S. J. *Polym. Sci., Polym. Symp.* **1971**, 19–30.

(75) Saito, M.; Yabe, A. *Text Res J* **1983**, *53*, 54–59.

(76) Bicerano, J. *Prediction of Polymer Properties*, 3rd ed.; Marcel Dekker: New York, 2002.

(77) Dann, J. R. *J. Colloid Interface Sci.* **1970**, *32*, 302–320.

(78) Noskov, S. Y.; Lamoureux, G.; Roux, B. *J. Phys. Chem. B* **2005**, *109*, 6705–6713.

(79) Hubbard, A. T. *Encyclopedia of Surface and Colloid Science*; Marcel Dekker: New York, 2002.

(80) Weissenborn, P. K.; Pugh, R. J. *J. Colloid Interface Sci.* **1996**, *184*, 550–563.

(81) Schwarcz, A.; Farinato, R. S. *J. Polym. Sci., Part B: Polym. Phys.* **1972**, *10*, 2025–2031.

(82) Kaelble, D. H.; Cirlin, E. H. *J. Polym. Sci., Part A: Polym. Chem.* **1971**, *9*, 363–368.



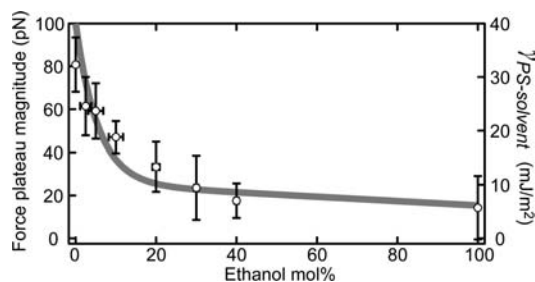


**Figure 3.** Plateau force magnitude and interfacial free energy as a function of the mol % ethanol in water. The open circles with error bars are calculated from the experimental force plateau data. The vertical errors are due to the cantilever thermal noise and standard deviation in the results for multiple samples; the horizontal error bars come from the precision of preparing and maintaining the correct ethanol concentrations (as a result, zero error bars for pure water and pure ethanol). The thick gray line is the calculated polymer–solvent interfacial free energy at various ethanol concentrations.

**Table 3.** Plateau Force Magnitude and Interfacial Free Energy in Pure Water and 2 M NaCl Solution

	pure water	2 M NaCl solution
interfacial free energy (mJ/m <sup>2</sup> )	40.0	43.6
plateau force (pN)	80 ± 13	97 ± 15

To show that a single polystyrene chain is being pulled, over 300 force–extension curves were superposed (Figure 4a) from uncorrelated locations on the surface. Discrete force plateaus at integral multiples of ~80 pN (Figure 4b) were observed and interpreted as pulling of multiple chains in parallel.<sup>83</sup> This strongly indicates that the lowest force step corresponds to the pulling of a single chain. The force magnitude of the lowest plateau was used for different solvent conditions in this report.

We observed that the transition from plateau to entropic elastic behavior in the high surface tension aqueous solvents

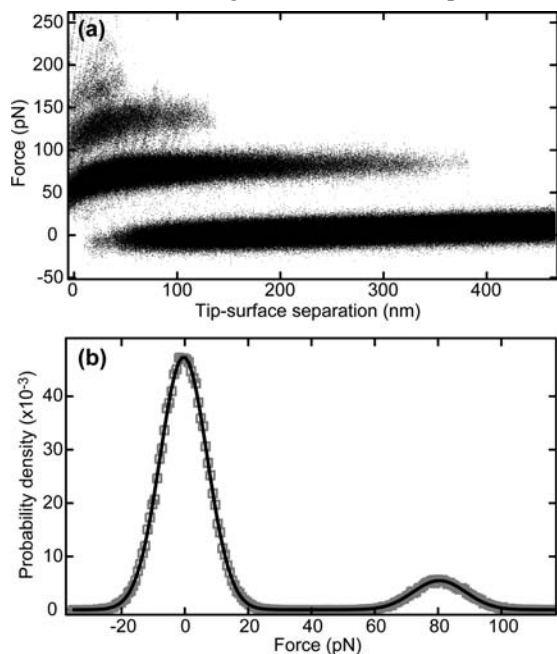


**Figure 4.** (a) Superposition of ~300 force–extension curves shows discrete steps, which indicates the pulling of single chain from the surface. (b) Histograms (gray open squares) showing the baseline and the first step from the figure in (a) above. Gaussian distribution (solid black) fits well over the histogram. The taller peak on the left corresponds to the baseline, whereas the one on the right is the distribution of the first plateau forces.

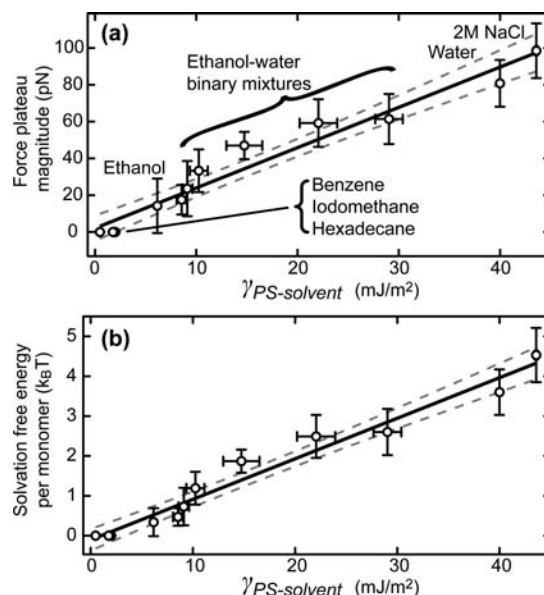


**Figure 5.** (a) Force plateau magnitude plotted against the interfacial energy between the solvent and polystyrene for various solvents. (b) Solvation free energy per monomer calculated from force plateau corrected for chain entropic elasticity. The linear fit and the 95% confidence interval of the fit are shown as solid and dashed lines, respectively.

such as pure water and NaCl solution is more distinct than for those in higher concentrations of ethanol. This suggests that the collapsed and extended structures are more distinct in higher surface tension aqueous solutions (e.g., pure water and salt solutions) than in low surface tension solutions (e.g., high ethanol concentration). It has been shown that polystyrene swells slightly<sup>84</sup> in ethanol while remaining in the collapsed state. Since the driving force for polystyrene to collapse in water is much greater than in ethanol solutions due to higher interfacial free energy, the collapsed structure should be more tightly condensed. Compared with well-collapsed polystyrene in water, the swelling in ethanol gives the polystyrene chain a conformation closer to that of an extended structure because more chains are solvent-exposed in the swelled state. This could contribute to the observed, more gradual transition from force plateau to entropic elasticity in ethanol.

**Single-Molecule Pulling of Polystyrene in Good Solvents.** Due to the incompatibility between the material of our microscope and good solvents for polystyrene such as tetrahydrofuran and toluene, we quote previous results for polystyrene pulling in toluene.<sup>85</sup> It has been shown that polystyrene force–extension profile agrees well with models describing entropic elasticity such as the freely joined chain model. This is not surprising, as one would expect this type of behavior for a homopolymer in good solvent. Because benzene, toluene, hexadecane, and iodomethane are all good solvents for polystyrene, it is reasonable to assume that the force–extension profile in all four solvents exhibit similar entropic elastic response. Therefore, we assigned a magnitude of zero to the hypothetical force plateau in these solvents.

**Correlation between Extension Force and Interfacial Free Energy.** Figure 5a plots the plateau force against the interfacial

(83) Thormann, E.; Simonsen, A. C.; Hansen, P. L.; Mouritsen, O. G. *Langmuir* **2008**, *24*, 7278–7284.

(84) Bernardo, G.; Vesely, D. *Eur. Polym. J.* **2007**, *43*, 938–948.

(85) Gunari, N.; Balazs, A. C.; Walker, G. C. *J. Am. Chem. Soc.* **2007**, *129*, 10046–10047.

free energy in different solvents. While benzene, hexadecane, and iodomethane (on the very low end of interfacial free energy) are good solvents for polystyrene, the rest of the solvents used in this study, which includes ethanol, ethanol–water mixture, water, and salt solutions, are bad solvents. The general trend is that the worse the solvent, the higher the plateau force. The data are well fitted by a line that passes through the origin, within the margin of error:

$$F_{\text{plateau}} = (2.2 \pm 0.3)\gamma_{\text{PS-sol}} + (2 \pm 7) \text{ [pN]} \quad (15)$$

where  $\gamma_{\text{PS-sol}}$  is in unit of  $\text{mJ/m}^2$ , the errors correspond to 95% confidence interval. This result strongly indicates the dependence of the magnitude of force plateau on the polymer–solvent interfacial free energy. The values are comparable to results from the analytical model introduced above ( $1.5\gamma_{\text{PS-sol}} + 2.4 \text{ pN}$ ), which assumed a flexible cylindrical hydrophobic polymer with dimensions estimated from the size of a styrene molecule. Of course, the assumption of the cylindrical polymer shape gives only a crude approximation of the solvent exposure area per polymer unit. However, the linear dependency and the similar values between experiment and theory show that the basic physics behind the force plateau is captured by the model.

Since the polymer conformation at the force plateau is balanced between collapsed and extended structures, the major contribution to the solvent exposure area comes from the extended portion of the chain. Because of entropic elasticity, the end-to-end distance of the chain is not the contour length of the chain, and since the surface exposure area is dependent on the contour length of the extended structure, the solvation free energy per monomer unit must be calculated using the contour length (Figure 2a). Using the worm-like-chain (WLC) model, we calculated the end-to-end length to contour length ratio (aka extension percentage) at each plateau force. The ratio ranges from 79% for higher forces to 40% for lower forces. The solvation free energy per monomer can be estimated by:

$$E_m = \frac{F_{\text{plateau}}d}{N} = F_{\text{plateau}}\frac{d}{L_c}l_m \quad (16)$$

where  $E_m$  is the solvation free energy per monomer,  $F_{\text{plateau}}$  is the plateau force,  $d$  is the end-to-end distance of the extended portion of the polymer,  $N$  is the number of units in the extended polymer,  $L_c$  is the contour length of the extended portion, and  $l_m$  is the length of each monomer. With this conversion, the solvation free energy is calculated and plotted against the interfacial free energy as shown in Figure 5b. The linear fit provides an estimate of the solvation free energy per monomer  $E_m$  (in unit  $k_B T$ ) given the interfacial free energy  $\gamma_{\text{PS-sol}}$  between the polymer and the solvent:

$$E_m = (0.10 \pm 0.01)\gamma_{\text{PS-sol}} - (0.1 \pm 0.3) \text{ [}k_B T\text{]} \quad (17)$$

where  $\gamma_{\text{PS-sol}}$  has a unit of  $\text{mJ/m}^2$  and assuming a monomer unit length of 0.24 nm, which corresponds to two C–C bond lengths at an angle of  $104^\circ$ . The errors here are calculated for a 95% confidence interval.

As mentioned above, in the water–ethanol and water–salt systems, the change in interfacial energy is mainly due to the polar and hydrogen-bonding interactions of the solvent alone, while the solvent–polymer and polymer–polymer self-interaction energies remain relatively constant. The dependence of the plateau force on the interfacial energy then suggests that the

plateau forces are direct results of “hydrophobic” interaction at fixed room temperature. This also suggests that the net effect of water structure at the microscopic interface with the hydrophobic polystyrene is already incorporated in the macroscopically measured interfacial free energy parameter. This knowledge could help reduce the complexity of simulations by showing that explicit water solvent may not be necessary for cases whose only concerns are hydrophobic hydration and hydrophobic interaction at fixed temperature.

A similar solvent-dependent study reported a linear dependence of the unbinding force between hydrophobic small molecules:  $\beta$ -cyclodextrin and adamantane on the surface tension of the solvent instead of the interfacial free energy.<sup>65</sup> For highly hydrophobic solute in alcohol–water mixtures, the interfacial free energy scales relatively linearly with the surface tension of the solvent due to linear scaling of the dispersive contribution of the solvent and the lack of polar contribution of the solutes. Hence, a linear correlation between force and interfacial free energy would also result in linear correlation between force and surface tension. However, the interfacial free energy is a more fundamentally significant parameter because it incorporates not only solvent–solvent interaction (surface tension), but also solvent–solute and solute–solute interactions. This is evident from the zero y-intercept of force–interfacial free energy plot and nonzero y-intercept<sup>65</sup> when graphing force against solvent surface tension. Therefore, it is more meaningful to use the interfacial free energy to explain hydrophobic and the more general solvophobic interaction. Furthermore, interfacial free energy is a more general description of the interaction between polymer and solvent and therefore can also be extended to explain polymers in good solvents. For example, iodomethane is a good solvent for polystyrene with an interfacial free energy value of  $0.5 \text{ mJ/m}^2$  but has a high surface tension value of  $45 \text{ mJ/m}^2$ . This places the force vs interfacial free energy data point of iodomethane on the line extrapolated from Figure 5a and b, but the iodomethane data point of force vs surface tension would not lie on any line that extrapolates force against surface tension.

**Force Plateau Is Due to Forced Solvation of Polymer in Poor Solvent.** Force plateaus in force–extension profiles have been observed in many polymer-pulling experiments; depending on the system, two mechanisms could lead to such force plateaus.<sup>83,86–91</sup> The first mechanism is due to polymer–surface interaction: a polymer is adsorbed onto the surface to form a train-like structure, and hence, the work of adhesion is proportional to the length of the polymer.<sup>86,88–90,92</sup> The polymers can form train-like structures when dissolved in good solvent,<sup>86</sup> implying that the adsorbed polymer has an extended conformation on the surface. The literature that reports such train-like structures usually uses polymers that are charged, making the desorption force sensitive (change up to 2 orders of magnitude) to relatively small changes in the ionic concentration (in 5–100 mM range).<sup>88,89,91</sup> The second mechanism for observed plateau force is due to force-induced solvation of polymer chains in

(86) Cui, S. X.; Liu, C. J.; Wang, Z. Q.; Zhang, X. *Macromolecules* **2004**, *37*, 946–953.

(87) Scherer, A.; Zhou, C. Q.; Michaelis, J.; Brauchle, C.; Zumbusch, A. *Macromolecules* **2005**, *38*, 9821–9825.

(88) Hugel, T.; Grosholz, M.; Clausen-Schaumann, H.; Pfau, A.; Gaub, H.; Seitz, M. *Macromolecules* **2001**, *34*, 1039–1047.

(89) Hugel, T.; Seitz, M. *Macromol. Rapid Commun.* **2001**, *22*, 989–1016.

(90) Liu, C. J.; Shi, W. Q.; Cui, S. X.; Wang, Z. Q.; Zhang, X. *Curr. Opin. Solid State Mater. Sci.* **2006**, *9*, 140–148.

(91) Seitz, M.; Friedsam, C.; Jostl, W.; Hugel, T.; Gaub, H. E. *Chem-PhysChem* **2003**, *4*, 986–990.

(92) Alvarez, J.; Whittington, S. G. *J. Stat. Mech.-Theory E* **2009**; 04016.



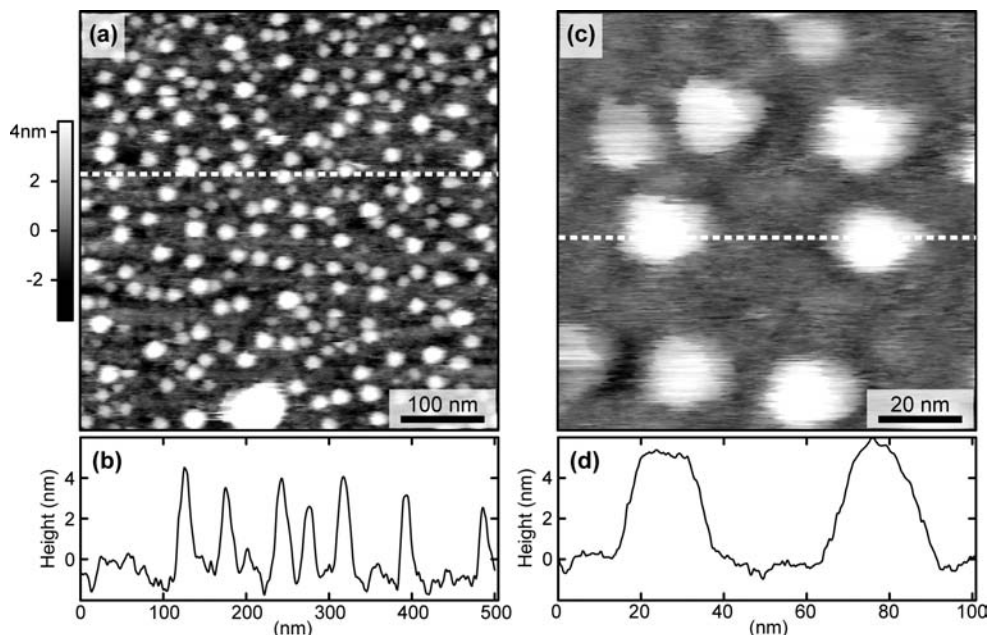


**Figure 6.** Surface topography of polystyrene deposited on Si surface. (a) Surface topography of a 500 nm  $\times$  500 nm area. (b) Cross-sectional profile of the white dashed line in (a). (c) Surface topography of a 100 nm  $\times$  100 nm area. (d) Cross-sectional profile of the white dashed line in (c).

poor solvents.<sup>83,87</sup> For the solvent-effect-induced force plateaus, two types of multiple force plateaus were observed: a constant step-size plateau implies pulling multiple noninteracting chains into the solvent,<sup>83</sup> whereas a nonconstant step-size plateau implies pulling polymer bundles into the solvent.<sup>87</sup> The force plateau reported here is due to the second mechanism (solvating polymer in poor solvent) for the following reasons.

First, the polystyrenes we studied are in poor solvents; therefore, it is unlikely that polystyrene assumes an extended state on the surface. A surface topography scan of sparsely deposited polystyrene (Figure 6a, c) shows that individual polystyrene molecules are indeed in their collapsed state with an average height of roughly 4–5 nm (Figure 6b, d), which is similar to the diameter of a single collapsed polystyrene at 7.3 nm as calculated from the specific volume of polystyrene below its glass transition temperature.<sup>93,94</sup>

$$\begin{aligned} v &= v_g - 2.5 \times 10^{-4}(T_g - T) \quad T < T_g \\ v_g &= 0.943 + 2.4 \times 10^{-4}T_g \\ T_g &= 100 - 1.7 \times 10^5/M \end{aligned} \quad (18)$$

where  $v$  (mL/g) is the specific volume of the polymer at temperature  $T$  ( $^{\circ}$ C),  $v_g$  (mL/g) is the specific volume at glass transition temperature  $T_g$  ( $^{\circ}$ C), and  $M$  is the molecular weight. The width of each dot is roughly 20 nm (Figure 6d) due to surface features convoluted with tip radius (average of 13 nm according to manufacture specification); the width after deconvolution is on the order of 5–10 nm, consistent with the height measurement. The uniformity in height and the size of the dots suggests that these are single polystyrene molecules in their collapse states on the Si surface.

Second, polystyrene is not charged; it should not respond directly to the ionic strength of the solvent as charged polymers do. The increase in plateau force at higher salt concentration is therefore a result of the increased solvent–solvent interaction,

**Table 4.** Force Plateau Magnitude Using Different Tip–Surface Combinations

tip–surface	Au–Au	Si <sub>3</sub> N <sub>4</sub> –Au	Si <sub>3</sub> N <sub>4</sub> –Si
force plateau magnitude	76 $\pm$ 10 pN	81 $\pm$ 16 pN	81 $\pm$ 13 pN

in line with the mechanism of solvating hydrophobic polymer in poor solvents.

Third, the plateau force observed in this report was found to be insensitive to the surface properties. Experiments performed on silicon (Si) and gold (Au) surfaces using silicon nitride (Si<sub>3</sub>N<sub>4</sub>) and gold-coated AFM tips showed no differences in the magnitude of the force plateau (see Table 4). Similarly, an experiment pulling polystyrene beads from hydrophilic and hydrophobic surfaces<sup>83</sup> also confirms that the plateau force is surface independent and is due to polymer–solvent interactions only. The force plateau magnitude in our study is dependent only on the solvent condition, which further confirms that the force plateau is the result of solvating polymer in poor solvents.

Last, depending on the deposition density of polystyrene on the surface, we obtained different multiple force plateaus with either a constant step size that corresponds to multiple noninteracting chains or step sizes that correspond to bundles or multiple chains, corresponding to the two polymer–solvent interaction scenarios described by previous experiments.<sup>83,87</sup>

#### Velocity Independence and Reversibility of Plateau Force.

To see whether the force plateau exhibits any sort of energy barrier crossing process, constant velocity pulling experiments at different pulling velocities were accomplished. Hundreds of force–extension curves for each pulling velocity were recorded. The force curves are then overlapped to generate a histogram of forces through the entire force–curve trajectory. By multiple peak fits with Gaussians, three major force populations were identified, coming from: (1) cantilever approaching the surface, (2) pulling on a single chain, and (3) retraction of the tip after the polymer desorbs from the tip. The first and third force populations are forces due to the hydrodynamic drag of the AFM cantilever. The force difference between the approach and retraction increases linearly with the pulling velocity. The linear

(93) Fox, T. G.; Flory, P. J. *J. Appl. Phys.* **1950**, *21*, 581–591.

(94) Liu, C. Y.; Morawetz, H. *Macromolecules* **1988**, *21*, 515–518.

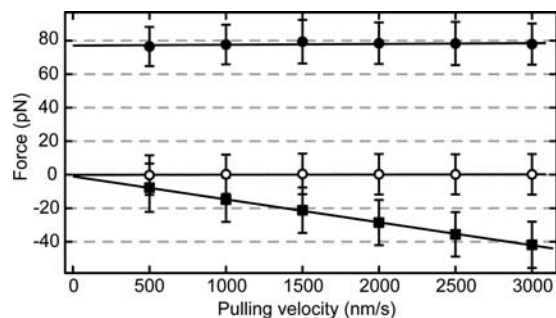


**Figure 7.** The force plateau magnitude (solid circles) is velocity independent from 500 to 3000 nm/s. The retraction portion (hollow circles) of the force curves are zeroed as the reference because the cantilever is moving at the same velocity in the same direction in this region as the force plateau region. The hydrodynamic drag of the cantilever can be clearly seen from the surface approaching portion (solid squares) of the force curve. Solid lines are linear fits to each of the three data sets. There is no apparent velocity dependency of the force plateau magnitude within the margin of error. Also note the linear dependency of hydrodynamic drag to velocity, indicating the flow of solvent around the cantilever is laminar.

dependence of the two also indicates that the water flow around the cantilever is laminar, giving minimal turbulence to the system. When a single chain is pulled, because a force plateau region is reached, the velocity of the cantilever is the same as after the polymer desorbs from the cantilever. Hence, the hydrodynamic contribution in this region of the force curve is equal to that during the free retraction. To see whether there is a pulling velocity dependency, the free retraction was chosen as the reference force and plotted the magnitude of the forces against pulling velocity. Figure 7 shows that both force populations that correlate to single and double chain pulling are constant through the range of velocity.

We do not observe activated barrier-crossing processes in these experiments performed at constant room temperature (300 K). If the process were to involve cantilever force-driven barrier-crossing events, a larger plateau force, or even a random sawtooth pattern, would be expected as the pulling velocity is increased. This has been well explored and documented in protein unfolding and dissociation of binding partners.<sup>58,95,96</sup> Unlike protein unfolding where a significant energy barrier is crossed going from folded to unfolded state, the free energy landscape of extending polystyrene in poor solvents seems to be monotonically increasing. However, one could imagine that it is possible that the free energy landscape is rugged due to the hydration energy of each polymer unit as each is being pulled out of the collapsed globule. This barrier does not exist in the continuum model for a polymer that looks like spaghetti. However, if one were to consider the polymer made of finite-sized beads and each bead were exposed to the solvent in an on/off fashion, then a small finite barrier would exist per monomer. These small barriers contribute to a staircase-like roughness on the overall monotonically increasing energy landscape as illustrated by the gray line in Figure 8. The linear spring constant of the AFM cantilever gives rise to a parabolic energy landscape (Figure 8, dashed line). When the polymer system is coupled to the AFM cantilever, the energy landscape of the system is the sum of the previous two (Figure 8, black line). This shifts the system's energy minimum to a lower end-to-end distance from the cantilever's intrinsic equilibrium position, which is interpreted as the deflection of the cantilever.

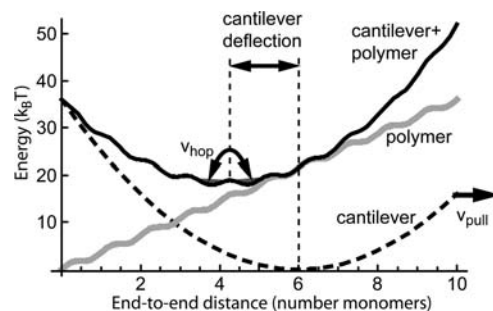


**Figure 8.** Schematic of the energy landscape of the polymer, the AFM cantilever, and the polymer–cantilever system along the coordinate of end-to-end distance of the polymer. The end-to-end distance of the polymer equals the surface–tip distance of the AFM cantilever when the polymer is attached to the tip.

Due to the roughness on the polymer's own energy landscape, there will be roughness at the bottom of the system's energy landscape, which is populated according to Boltzmann's distribution. Therefore, as long as the lowest-energy states are populated much faster than the rate at which the cantilever pulls on the polymer, i.e.  $v_{\text{hop}} \gg v_{\text{pull}}$  (Figure 8), there will be no observable force dependency on the pulling velocity that is caused by the roughness of the energy landscape. The barrier height is roughly  $1.1 k_B T$ , which is close enough to the thermal noise floor, and allows a fast hopping rate from one minimum in the energy landscape to an adjacent one.

The pulling velocities ranging from 500 to 3000 nm/s in these experiments are probably too slow to probe significant barrier-crossing events. The time scale required to see the dependence of force on velocity would depend on the diffusion constant of the polystyrene in solvent as well as the barrier height (in this case, the solvation free energy per monomer).

We find that the time scale of our pulling experiment is also slower than the self-organization time scale of the collapsed state. The portion of the polystyrene in the collapsed state has enough time to rearrange itself to avoid self-entanglement or is initially not entangled. Supposing that the collapsed state of polystyrene could not rearrange fast enough compared to configurational changes induced by the pulling, we would unavoidably pull entangled polystyrene out of the collapsed state. The force–extension profile of such events would neither have a constant force profile due to trapped states, nor be velocity independent due to friction between polymer chains. The behavior of such a scenario would be similar to plastic deformation. Last, the velocity independence also excludes the possibility that the force plateau is due to hydrodynamic friction between the polymer and the solvent. Any friction between polymer and solvent is due to hydrodynamic drag, which would exhibit a pulling-rate dependency. All of the above evidence further suggests that the behavior of the polymer system is due to a conformation transition from collapsed state to extended state in poor solvent and that the magnitude of the extension force is a result of the solvent condition.

We cycled among polymer states by moving the AFM tip back and forth above the surface before the chain breaks off from the tip. We find the force curves are reversible in both directions, indicating that the process is reversible. Again, the time scale of the experiment is much greater than the dynamics

(95) Zhang, X.; Liu, C. J.; Wang, Z. Q. *Polymer* **2008**, *49*, 3353–3361.

(96) Evans, E.; Ritchie, K. *Biophys. J.* **1997**, *72*, 1541–1555.

of the chain; hence, the system is in equilibrium with its surroundings.

### Conclusion

In this paper, the force–extension behavior of a hydrophobic polymer in aqueous solutions by single-molecule force spectroscopy was examined in detail. The force–extension curve shows a constant force plateau region as predicted by our model based on the established idea that collapsed and extended components coexist on a hydrophobic polymer under tension. The dependency of the extension force on the solvent condition was examined using ethanol–water and salt–water solutions that shows a linear dependence of the extension force to the interfacial free energy between the polymer and the solvent. The majority of the changes in interfacial free energy in our experiment are due to changes in polar and hydrogen-bonding interactions of the solvent. The linear transition of the polymer extension force in pure water to that of pure ethanol indicates that the hydration of hydrophobic polymer in pure water transitions smoothly to the more general solvophobic effect. This may suggest that hydrophobic effect is essentially solvophobic effect with water as the main solvent. The linear fit intersects the origin of the plot corresponding to the zero interfacial energy and zero solvation free energy, where purely entropic elasticity response for the polymer in good solvent is expected. The correlation between the microscopic solvation free energy per

monomer unit and the macroscopic interfacial free energy implies that the macroscopically measured interfacial free energy has a corresponding counterpart on the microscopic level. This suggests that the interfacial free energy alone is enough to describe the behavior of polystyrene in various solvents at fixed temperature and that the special properties of water such as the hydrogen-bonding structure are likely already incorporated in the interfacial free energy value. Finally, the force–extension profile was found to be independent of pulling velocity, which confirms that the plateau force observed is due to hydrophobic hydration and not polymer plasticity or polymer–solvent friction.

**Acknowledgment.** We thank Prof. S. G. Whittington for insightful discussions and critical comments on the manuscript, Dr. Weiqing Shi and Dr. Nikhil Gunari for their consistent support throughout the project, and lastly Ruby May A. Sullan and James K. Li for helpful feedback on the manuscript. This research was financially supported by Natural Science and Engineering Research Council of Canada (NSERC), the National Science Foundation (NSF), and the Office of Naval Research (ONR).

**Supporting Information Available:** A derivation of the analytical model and numerical solution method. This material is available free of charge via the Internet at <http://pubs.acs.org>.

JA101155H